Available online at www.sciencedirect.com

SciVerse ScienceDirect

Ceramics International 39 (2013) 5591–5596

CERAMICS INTERNATIONAL

www.elsevier.com/locate/ceramint

Thermal shock resistance of a ZrB_2–SiC–graphite composite in low oxygen partial pressure environment

Hua Jin*, Songhe Meng, Qiang Yang, Yanwei Zhu

Science and Technology on Advanced Composites in Special Environments Laboratory, Harbin Institute of Technology, Harbin 150001, China

Received 21 November 2012; received in revised form 8 December 2012; accepted 8 December 2012
Available online 26 December 2012

Abstract

The heating rate and size effect on thermal shock resistance of a ZrB_2–SiC–graphite (ZSG) composite was studied by measuring the retention of the flexural strength after rapid resistance heating in a low oxygen partial pressure environment. The residual strength values for the specimen heated in a low oxygen partial pressure of 200 Pa decreased gradually as the temperature increased under high heating rate of 200 °C/s, 300 °C/s and 500 °C/s, and then increased suddenly when the temperature reached 1800 °C. The residual strength values for the specimen with heating rate of 200 °C/s were obviously greater than others and approximate that of the original specimen. At a temperature above 1800 °C, the residual strength decreased again with increasing temperature under different heating rate. Furthermore, the size effect on thermal shock at different temperature was investigated. The experimental results revealed that thermal shock resistance of the ZSG composite was sensitive to the heating rate and size effect. The microstructure of the ZSG composite in different conditions were also presented and analyzed.

Keywords: A. Hot pressing; B. Composites; C. Thermal shock resistance; C. Strength

1. Introduction

Zirconium diboride (ZrB_2) based ultrahigh temperature ceramics are considered candidates as potential materials for a variety of high temperature structural applications [1–5]. The addition of appropriate amounts of SiC particles not only enhances the mechanical properties, but also improves the oxidation resistance of ZrB_2 by promoting the formation of silicate-based glasses that inhibit oxidation at temperatures between 800 and 1800 °C [6–8]. Although the ZrB_2–SiC composite have many advantages, their intrinsic brittle characteristics induce poor thermal shock resistance and keep them from being widely used, especially for applications in the extreme environment. A lot of previous work indicates that incorporating the second phase additions such as fiber, flakes, and whiskers into the ZrB_2–SiC composite could obtain the higher aspect ratio to enhance the toughness [9–13]. In particular, the graphite flake introduced into the ZrB_2–SiC composite is an attractive material for high temperature applications. Because it can not only increase fracture toughness but also improve thermal shock resistance compared with the ZrB_2–SiC composite [14,15].

At present, the test methods available for measurement of the thermal shock resistance of ceramic matrix composites can be broadly classified into two groups: the thermal shock during heating and the thermal shock during cooling [16]. The water quenching is the most popular cooling thermal shock method in which the specimens are heated to a desired temperature, then quenched into water bath, and measured the flexural strength after that [17]. However, water quenching experiments could generate higher rates of heat transfer than it would experience during its actual use, and the heat transfer coefficient involved in a water quenching method is difficult to measure due to the vaporization of water. Moreover, this method is of little relevance for ZrB_2-based composites used in hypersonic vehicle, which suffered thermal shock of heating during aero-thermodynamic load [18]. Therefore, the heating thermal shock method could be more close to the actual conditions, and the resistance heating technique is more

---

*Corresponding author. Tel./fax: +86 451 8640 2432.
E-mail address: 2007hit@163.com (H. Jin).

0272-8842/$ - see front matter © 2012 Elsevier Ltd and Techna Group S.r.l. All rights reserved.
http://dx.doi.org/10.1016/j.ceramint.2012.12.074

considerable which is proposed for testing the thermal shock resistance of the ZrB_2–SiC composite. The research of thermal shock resistance focuses on influences of surface defects, indentation crack length, crack density, particle reinforced or whisker reinforced and glass phase on thermal shock resistance performance in water quenching experimental way. Only the effects of failure, repeated behaviors and oxidation on thermal shock resistance with electrical resistance heating method were reported. From the results of research, the thermal shock resistance performance of the ZSG composite is susceptible to the component geometry, thermophysics property, pressure and thermal loading conditions. So it is inappropriate to consider thermal shock resistance of the material only, the heating rate, size and pressure effect should be taken into account. However, up to date, no paper devotes to study on effect of thermal shock resistance for the ZSG composite using the electrical resistance heating technique in the low oxygen pressure environment, since the experiment is difficult to simulate the heating thermal shock in this environment. The oxygen partial pressure and chemical composition of the atmosphere can hardly be precisely controlled by present experiment set-up, such as arc jet.

Hence, in this study a heating thermal shock experiment using an electric resistance heating method for the ZSG composite is carried out, and the influence of temperature, heating rate and size effect are investigated. The purpose of this work is to study the effects of temperature, heating rate and size on thermal shock resistance of the ZSG composite in a low oxygen partial pressure by using home-made thermal shock set-up. Moreover, the microstructures of the ZSG composite after thermal shock experiments in different conditions were analyzed and discussed.

2. Experimental

Commercially available ZrB_2 powders (Northeast Institute for Non-ferrous Metal Research, China) had a purity of $>99.5\%$ and mean particle size of 5 μm. The SiC powders (Xuzhou Hongwu Nanometer Materials, China) had a reported purity of 98.5% and mean particle size of 2 μm. The graphite flake (Qingdao Tiansheng Graphite Co., Ltd., China) had a purity of 99.5% and mean diameter and thickness are 15 μm and 1.5 μm, respectively. The powder mixtures of ZrB_2 plus 20 vol% SiC plus 10 vol% graphite flake were ball-mixed for 10 h in a polyethylene bottle using ZrO_2 balls and ethanol as the grinding media. After mixing, the slurry was dried in a rotary evaporator and screened. The resulting powder mixtures were hot-pressing at 1900 °C for 1 h under a uniaxial load of 30 MPa in Ar atmosphere. The specimens were prepared by cutting cross sections parallel to the hot-pressing direction and then polishing to 2 μm using diamond abrasives. The flexural strength of the specimen before and after the thermal shock was measured in three-point bending on 3 mm × 4 mm × 36 mm and 6 mm × 8 mm × 36 mm bars, with a 30 mm span and a crosshead speed of 0.5 mm/min. A minimum number of six specimens were measured for per experimental condition. The edges of all the specimens were chamfered to minimize the effect of stress concentration due to machining flaws. The thermal shock resistance was measured by a home-made high current electrical set-up with maximum power of 50 kW as shown in Fig. 1. Oxygen (> 99.99%) and argon (> 99.99%) were introduced by a nozzle into the environment reactor and oxygen partial pressure can be adjusted by controlling the flow rate ratio between oxygen and argon. Gas pressures in the environment reactor were measured and monitored by a digital pressure gauge with oxygen partial pressure of 200 Pa in constant. The linear increase in the temperature of the specimen was obtained by multi-wavelength pyrometer with measurement range of 1000–2200 °C, and the heating rate was 200 °C/s, 300 °C/s and 500 °C/s. The microstructure of the specimen after thermal shock was examined by using scanning electron microscopy (SEM; FEI Sirion, Holland) along with energy dispersive spectroscopy (EDS, EDAX, USA) for component analysis.

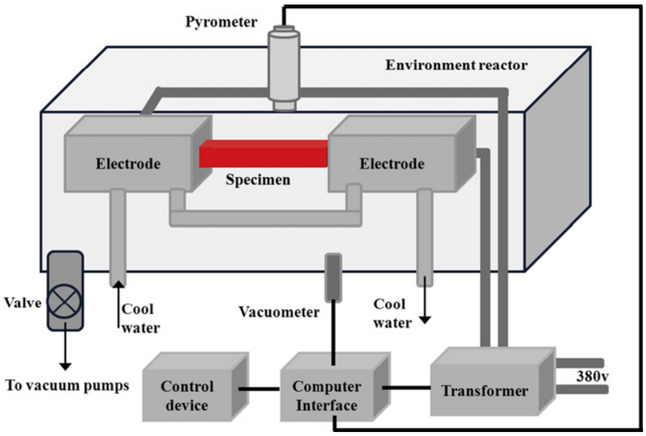

Fig. 1. Schematic diagram of home-made thermal shock set-up.

3. Results and discussions

Fig. 2 shows the change curve in temperature of the specimen center with increasing testing time with different heating rates. The maximum temperature (2200 °C) of the specimen center was obtained in 11.03 s, 7.37 s and 4.43 s for the heating rate of 200 °C, 300 °C and 500 °C. The specimen was cooled down to 1000 °C (because of the measuring range of multi-wavelength pyrometer) in 5.21 s, 6.75 s and 4.38 s, due to the different heating times and the coolant system.

The thermal shock resistance was evaluated through measuring the flexural strength after heating thermal shock; the residual strength of the specimen was plotted as a function of the heating temperature, as shown in Fig. 3. Compared with the original strength of 480 MPa, the residual strength showed a declining trend with temperature increase due to internal thermal stress resulted

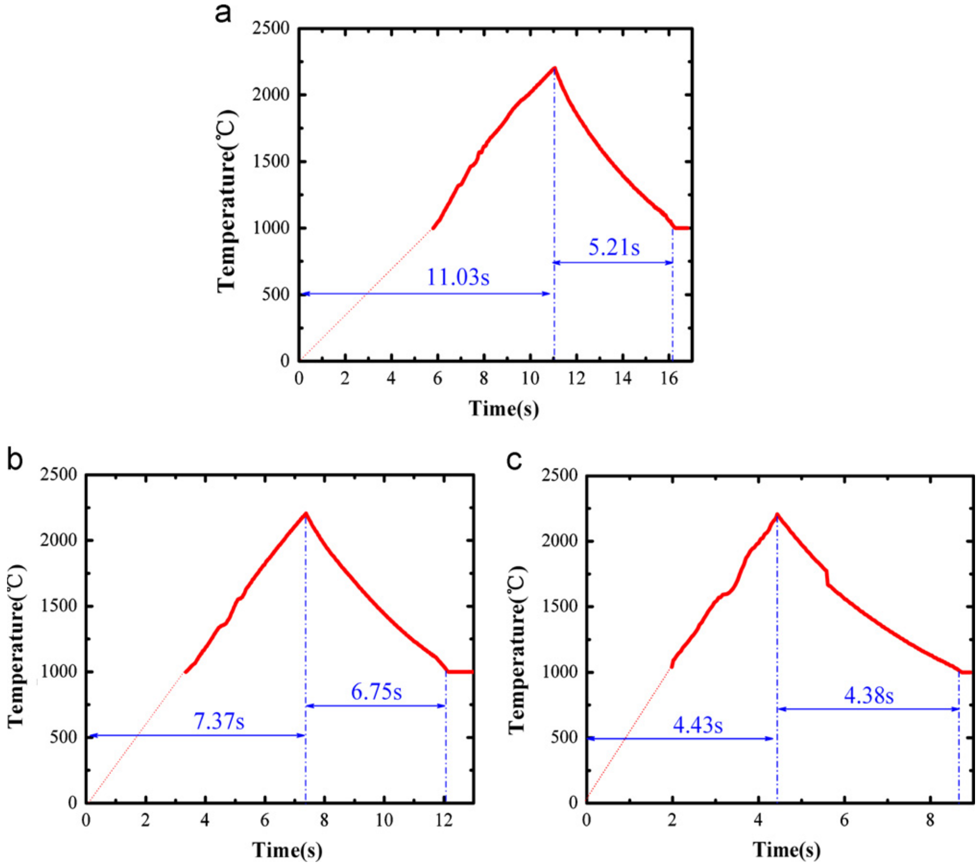

Fig. 2. The change curve of temperature of the specimen center vs. increasing testing time with (a) 200 °C/s; (b) 300 °C/s; (c) 500 °C/s.

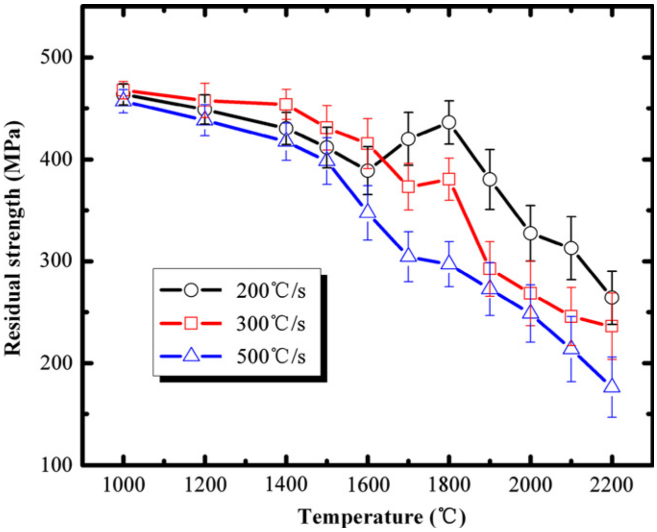

Fig. 3. Plot of the residual strength versus temperature with different heating rates in a low oxygen partial pressure.

from inhomogeneous temperature field. However, the residual strength increased suddenly when temperature reached 1800 °C, while the residual strength for the specimen with heating rate of 200 °C/s as high as 438 MPa was significantly improved. It was obviously higher than others and approximate that of the original specimen. When temperature was above 1800 °C, the residual strength decreased again with increasing temperature under different heating rates. This phenomenon was presumably attributed to the compression stress and the formation of the oxide layer that healed the flaws on the surface of the specimen. For heating rate of 500 °C/s, when the specimen was heated to 1800 °C the residual strength did not increase due to the heating time was too short to sufficiency oxidation. It could be seen from Fig. 3, the residual strength was reduced evidently with increase in heating rate and the shocked specimen with heating rate of 500 °C/s showed a minimal strength at every temperature, followed by 300 °C/s and 200 °C/s. It revealed that the thermal shock resistance was sensitive to the heating rate.

The surface of the ZSG composite was oxidized to oxides when it was exposed to air at high temperature, for example, ZrB_2 would be oxidized to ZrO_2 and B_2O_3 at above 650 °C [19]; SiC would be oxidized to SiO_2 and CO_2 at above 800 °C; Graphite would be oxidized to CO_2 [20]. So the expected main reactions were described as follows:

$$ZrB_2(s)+5/2O_2 \rightarrow ZrO_2(s)+B_2O_3(g) \tag{1}$$

$$SiC(s)+2O_2 \rightarrow SiO_2(l)+CO_2(g) \tag{2}$$

$$SiC(s)+3/2O_2 \rightarrow SiO(g)+CO_2(g) \tag{3}$$

$$SiO_2(l)+B_2O_3(l) \rightarrow SiO_2B_2O_3(l) \tag{4}$$

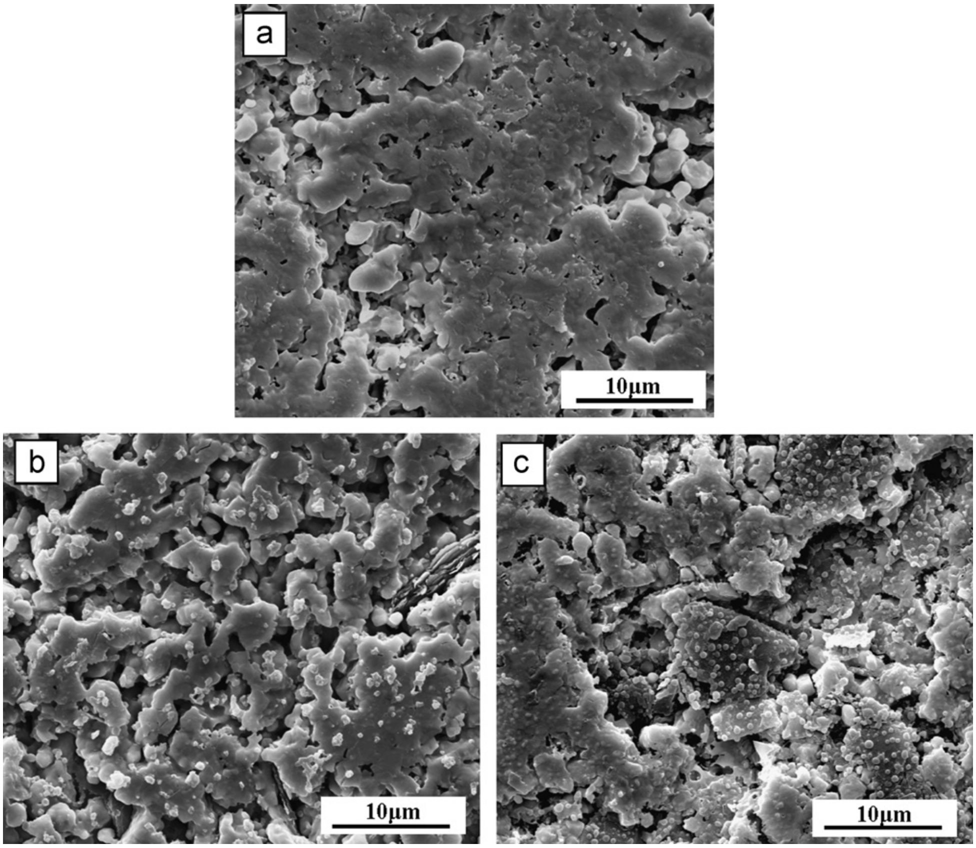

Fig. 4. Typical SEM micrographs of the ZSG composite for the heating rate of (a) 200 °C/s, (b) 300 °C/s, (c) 500 °C/s at 1800 °C.

$$C + O_2 \rightarrow CO_2(g) \tag{5}$$

$$ZrO_2(s) + SiO_2(l) \rightarrow ZrSiO_4(s) \tag{6}$$

$$ZrO_2(s) + SiO(g) + 1/2O_2 \rightarrow ZrSiO_4(s) \tag{7}$$

The surface microstructures of the ZSG composite after the thermal shock at 1800 °C with different heating rates were shown in Fig. 4. EDS analysis and XRD spectra (not shown here) documented that the white particles were ZrO_2 phase because the white particle was only composed of oxygen and zirconium elements, and a continuous glassy phase was SiO_2-rich glass that was expected to contain some B_2O_3 during transient heating to 1600 °C based on either incomplete evaporation of the B_2O_3 by reaction (3) or the continuous production of B_2O_3 beneath the outer scale by reaction (1) [19–21]. The $ZrSiO_4$ phase occurred while the thermal shock temperature was above 1200 °C. The probable formation routes of $ZrSiO_4$ phase were expressed in Eqs. (6) and (7), and the latter was related with the active oxidation of SiC, which was expressed as Eq. (3). The standard Gibbs energy of Eqs. (6) and (7) were calculated and it was noted that the Gibbs energy of zircon produced by the gaseous–solid reaction was lower than the reaction (6) and it decreased with increasing of oxidation temperature, while the formation energy calculated from Eq. (7) increased obviously at elevated temperatures. The lower formation energy indicated that the second route was preferred for the formation of zircon, and the formation of gaseous SiO was necessary. According to the volatility diagram of ZrB_2–SiC system calculated by Fahrenholtz [22], SiC exhibits preferential oxidation in the system of ZrB_2–SiC, and lower oxygen partial pressure led to the active oxidation of SiC under relatively lower temperature (as shown in Eq. (3)). In addition, the formation of protective silica film on the surface further lowered the oxygen partial pressure in the inner part, which aggravated the active oxidation of SiC. Hence formation of $ZrSiO_4$ by the second route was fulfilled with the participation of gaseous SiO_2. The surface flaws of the ZSG composite after the thermal shock increased as the heating rate increased, which was attributed presumably to the rapid change in the temperature of the surface of the specimen. The white ZrO_2 particles were covered with SiO_2-rich glass and the formation of such structure was presumably attributed to volume expansion and/or the mutual wetting behavior of the ZrO_2 and SiO_2-rich glass phases [22]. The surface micro-flaws were detrimental to the flexural strength of the specimen because ZrB_2-based ceramics were brittle and sensitive to the surface defects such as cracks and pores.

In order to investigate the effect of the surface flaws on the flexural strength of the specimen after the thermal

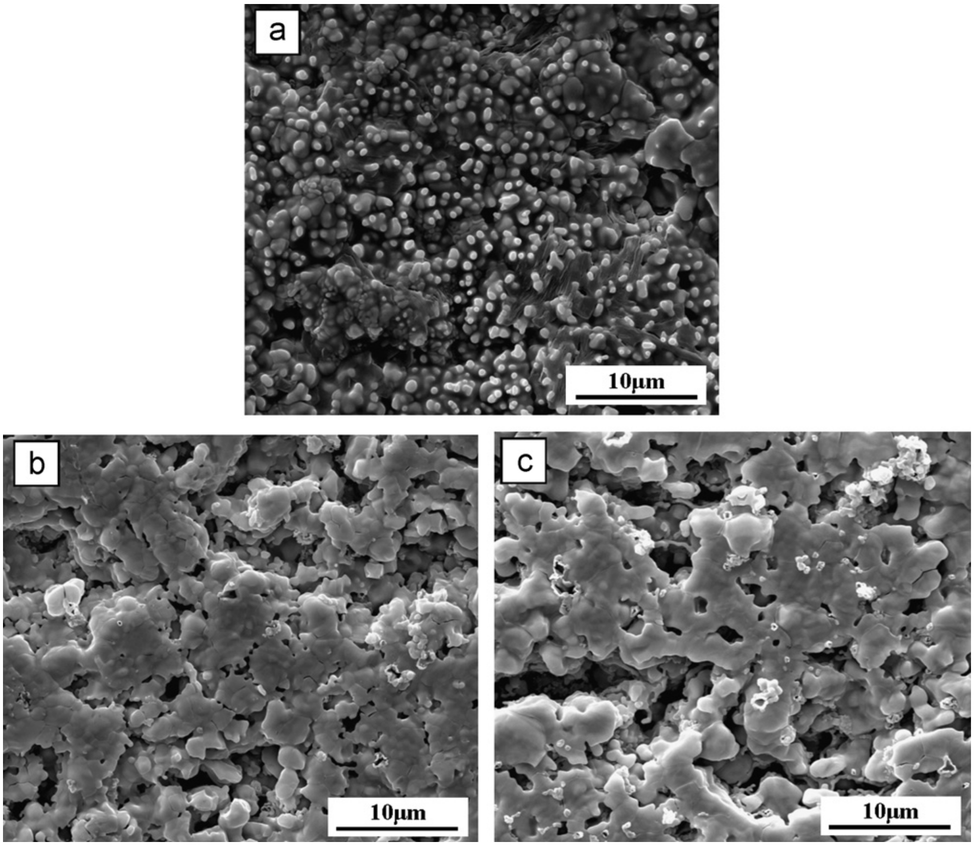

Fig. 5. Typical SEM micrographs of the ZSG composite for the heating rate of (a) 200 °C/s, (b) 300 °C/s, (c) 500 °C/s at 2200 °C.

shock, the surface microstructures of the ZSG composite after the thermal shock at 2200 °C with different heating rates were shown in Fig. 5. The circular ZrO_2 particles were formed on the surface of the specimen for heating rate of 200 °C/s and these particles were covered with SiO_2-rich glass. As the heating rate increased, the amount of ZrO_2 particle was reduced due to the reduction in time during high temperature and the amount of the surface flaw increased obviously. The change in surface microstructure resulted in the change of the flexural strength.

Fig. 6 showed the residual strength of the ZSG composite in two different sizes as a function of thermal shock temperature with heating rate of 300 °C/s. The residual strength for large size (6 mm × 8 mm × 36 mm) was lower than the small size (3 mm × 4 mm × 36 mm) at each temperature, where the maximum and minimum of reduction rate were 5.4% at 1200 °C and 55.6% at 2200 °C. The residual strength slowly increased at 1700 °C, which was different from small size how increased at 1800 °C. These results indicated that a strong size effect on the thermal shock resistance could be observed as a result of the difference in the characteristic thermal stress, which was different from size effect on the thermal shock behaviors by the water quenched method. The size effect was presumably due to two reasons: one was the thermal stress resulted from inhomogeneous temperature filed, which could provide the more crack initiation and propagation. Comparing the two scales we could see that the thermal stress became larger when the breadth and thickness of the specimen increased, as the effect of the thermal stress in breadth direction could not be ignored. The other was the areas of micro-cracks, which expanded as thermal stress increased for the large size. Furthermore, the residual stress after the thermal shock, which attributed to the difference in thermal expansion coefficient of components, could not be ignored for the size effect. It was rather remarkable that we could not improve the thermal shock behavior of the composites by decreasing size, because size was decided by the application.

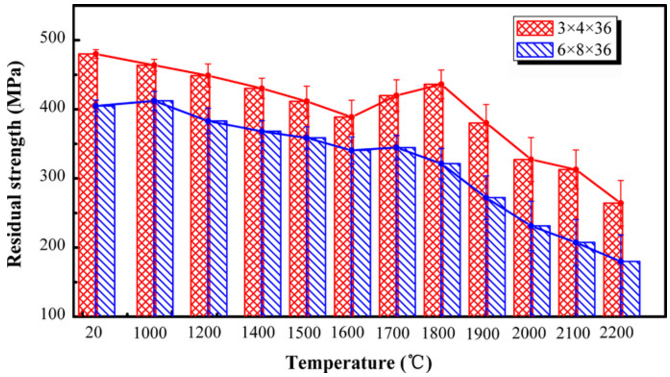

Fig. 6. Plot of the residual strength versus temperature with two sizes of specimens.

4. Conclusions

In conclusion, the effects of temperature, heating rate and size on thermal shock resistance of the ZSG composite were investigated using an electric resistance heating method, and the microstructures of the ZSG composite after thermal shock experiments in different conditions were analyzed and discussed. The maximum temperature (2200 °C) of the specimen center was obtained in 11.03 s, 7.37 s and 4.43 s for the heating rate of 200 °C, 300 °C and 500 °C. During the heating period, the macro-scale temperature field was not uniform and the specimen surface was oxidized when it was exposed to rarefaction oxygen at high temperature. The thermal shock resistance was evaluated through measuring the flexural strength after heating thermal shock. Compared with the original strength of 480 MPa, the residual strength showed obviously a decrease trend with temperature increased due to internal thermal stress because of inhomogeneous temperature field. However, the residual strength increased suddenly when temperature reached 1800 °C, while the residual strength values for the specimen with heating rate of 200 °C/s as high as 438 MPa improved significantly, and the residual strength reduced evidently with increase in heating rate and the shocked specimen with heating rate of 500 °C/s showed a minimal strength at each temperature, followed by 300 °C/s and 200 °C/s. It was proved that the thermal shock resistance was sensitive to the heating rate. Furthermore, the strong size effect on the thermal shock resistance could be observed as a result of the difference in the characteristic thermal stress, which was different from size effect on the thermal shock behaviors by the water quenched method.

Acknowledgements

This work is supported by National Natural Science Foundation of China under Grants #90505015.

References

[1] Z.H. Lü, D.L. Jiang, J.X. Zhang, Q.L. Lin, Processing and properties of ZrB_2–SiC composites obtained by aqueous tape casting and hot pressing, Ceramics International 37 (2011) 293–301.

[2] V. Zamora, A.L. Ortiz, F. Guiberteau, M. Nygren, On the enhancement of the spark-plasma-sintering kinetics of ZrB_2–SiC powder mixtures subjected to high-energy co-ball-milling, Ceramics International, http://dx.doi.org/10.1016/j.ceramint.2012.11.001, in press.

[3] S.Q. Guo, Densification of ZrB_2 based composites and their mechanical and physical properties: a review, Journal of the European Ceramic Society 29 (2009) 995–1011.

[4] P. Sarin, P.E. Driemeyer, R.P. Haggerty, D.K. Kim, J.L. Bell, Z.D. Apostolov, W.M. Kriven, In situ studies of oxidation of ZrB_2 and ZrB_2–SiC composites at high temperatures, Journal of the European Ceramic Society 30 (2010) 2375–2386.

[5] A.L. Chamberlain, W.G. Fahrenholtz, G.E. Hilmas, D.T. Ellerby, Oxidation of ZrB_2–SiC ceramics under atmospheric and reentry conditions, Refractories Applications Transactions 2 (2005) 1–8.

[6] J. Zhou, G.J. Zhang, H. Zhang, Z.R. Huang, J. Vleugels, O.V. Biest, Improving high temperature properties of hot pressed ZrB_2-20 vol% SiC ceramic using high purity powders, Ceramics International 39 (2013) 871–876.

[7] S.Q. Gao, T. Mizuguchi, M. Ikegami, Y. Kagawa, Oxidation behavior of ZrB_2–$MoSi_2$–SiC composites in air at 1500 °C, Ceramics International 37 (2011) 585–591.

[8] J.C. Han, P. Hu, X.H. Zhang, S.H. Meng, Oxidation behavior of zirconium diboride–silicon carbide at 1800 °C, Scripta Materialia 57 (2007) 825-828.

[9] J. Lin, X.H. Zhang, W.B. Han, D. Sun, Influence of milling time on the synthesis, microstructure and mechanical properties of ZrB_2–SiC–ZrO_{2f} ceramic composites, Ceramics International, http://dx.doi.org/10.1016/j.ceramint.2012.11.003, in press.

[10] Y.G. Wang, M. Zhu, L.F. Cheng, L.T. Zhang, Fabrication of SiC_w reinforced ZrB_2-based ceramics, Ceramics International 36 (2010) 1787–1790.

[11] M. Ikegami, S.Q. Guo, Y. Kagawa, Densification behavior and microstructure of spark plasma sintered ZrB_2-based composites with SiC particles, Ceramics International 38 (2012) 769–774.

[12] W.M. Guo, Z.G. Yang, G.J. Zhang, Microstructural evolution of ZrB_2–MoSi composites during heat treatment, Ceramics International 37 (2011) 2931–2935.

[13] R.J. He, X.H. Zhang, P. Hu, C. Liu, W.B. Han, Aqueous gelcasting of ZrB_2–SiC ultra high temperature ceramics, Ceramics International 38 (2012) 5411–5418.

[14] Z. Wang, C.Q. Hong, X.H. Zhang, X. Sun, J.C. Han, Microstructure and thermal shock behavior of ZrB_2–SiC–graphite composite, Materials Chemistry and Physics 113 (2009) 338–341.

[15] Z. Wang, S. Wang, X.H. Zhang, P. Hu, W.B. Han, C.Q. Hong, Effect of graphite flake on microstructure as well as mechanical properties and thermal shock resistance of ZrB_2–SiC matrix ultra-high temperature ceramics, Journal of Alloys and Compounds 484 (2009) 390–394.

[16] P.K. Panda, T.S. Kannan, J. Dubois, C. Olagnon, G. Fantozzi, Thermal shock and thermal fatigue study of ceramic materials on a newly developed ascending thermal shock test equipment, Science and Technology of Advanced Materials 3 (2002) 327–334.

[17] X.H. Zhang, Z. Wang, C.Q. Hong, P. Hu, W.B. Han, Modification and validation of the thermal shock parameter for ceramic matrix composites under water quenching condition, Materials Design 30 (2009) 4552–4556.

[18] F. Monteverde, R. Savino, M.D.S. Fumo, A.D. Maso, Plasma wind tunnel testing of ultra-high temperature ZrB_2–SiC composites under hypersonic re-entry conditions, Journal of the European Ceramic Society 30 (2010) 2313–2321.

[19] T. Zhu, W.J. Li, X.H. Zhang, P. Hu, C.Q. Hong, L. Weng, Oxidation behavior of ZrB_2–SiC–ZrO_2 ceramic composites in the temperature range of 800–1200 °C, Materials Chemistry and Physics 116 (2009) 593–598.

[20] W.M. Guo, G.J. Zhang, Y.M. Kan, P.L. Wang, Oxidation of ZrB_2 powder in the temperature range of 650–800 °C, Journal of Alloys and Compounds 471 (2009) 502–506.

[21] D. Gao, Y. Zhang, C.L. Xu, Y. Song, X.B. Shi, Oxidation kinetics of hot-pressed ZrB_2–SiC ceramic matrix composites, Ceramics International, http://dx.doi.org/10.1016/j.ceramint.2012.09.091, in press.

[22] F. Monteverde, R. Savino, M.D.S. Fumo, Dynamic oxidation of ultra-high temperature ZrB_2–SiC under high enthalpy supersonic flows, Corrosion Science 53 (2011) 922–929.